Proceedings of Meetings on Acoustics

Volume 19, 2013 http://acousticalsociety.org/

ICA 2013 Montreal
Montreal, Canada
2 - 7 June 2013

Structural Acoustics and Vibration
Session 3aSA: Acoustic Metamaterials I

3aSA5. Experimental validation of the band-gap and dispersive bulk modulus behaviour of locally resonant acoustic metamaterials

Matthew Reynolds*, Yan Gao and Steve Daley

***Corresponding author's address: ISVR, University of Southampton, University Road, Southampton, SO17 1BJ, Hampshire, United Kingdom, mjr304@soton.ac.uk**

Over the last decade there has been significant interest in the design and production of acoustic metamaterials with physical qualities not seen in naturally occurring media. Progress in this area has been stimulated by the desire to create materials that exhibit novel behaviour such as negative refraction due to negative material parameters, and band gaps in the frequency response of the material. An acoustic metamaterial is presented that consists of an acoustically transparent mesh with an array of split hollow spheres. Split hollow spheres are analogous to the split ring resonators found in many electromagnetic metamaterials and act as Helmholtz resonators providing a resonant band gap at low frequencies where achieving a Bragg gap would be impractical, and providing a dispersive effective bulk modulus that can become negative. Since an eventual goal of the work is to produce such materials on a micro-scale, the metamaterial is designed for, and produced using, 3D printing techniques (additive layer manufacturing). Results are presented for material comparing theory and experiment, and methods for increasing the bandwidth of the behaviour in question are proposed, including a mixed resonator solution.

Published by the Acoustical Society of America through the American Institute of Physics

Received 22 Jan 2013; published 2 Jun 2013

INTRODUCTION

Over the last decade there has been significant research interest into the development of acoustic metamaterials and the novel behaviour they produce. Locally resonant periodic materials, called metamaterials, were first proposed in the electromagnetic domain by Smith [1] as a way of realising the 'left handed' behaviour first postulated by Vesalago many years earlier [2], where the implications of a material with simultaneously negative electromagnetic permeability and permittivity were presented. The analogy of acoustic and electromagnetic waves has led to a great deal of research into acoustic metamaterials [3, 4, 5], where the analogues of permeability and permittivity are density and bulk modulus respectively. When both become negative simultaneously (where the material is said to be in its double negative (DNG) region), the refractive index has a negative sign so negative refraction occurs. In this region Snell's law still applies, however the path of the reflected wave lies to the opposite side of the incident normal than one would expect in a regular transmission medium, and the group and phase velocity vectors are anti-parallel. Band gaps appear in the dispersion characteristics of metamaterials, at high frequencies due to Bragg scattering effects [4] related to the periodic properties of the material and, in materials where low frequency resonances occur, at frequencies around two orders of magnitude lower [5]. This leads to high levels of attenuation in the transmission characteristics of the material at these frequencies. These novel properties mean that metamaterials are of particular interest and have been proposed as a potential solution to achieve acoustic cloaking [6], transmission blocking [7] and subwavelength acoustic lenses [5].

This paper presents experimental validation of a 1 dimensional acoustic metamaterial consisting of an array of split hollow spheres (SHS) suspended in an acoustically transparent mesh. Whilst there are not many real world environments where 1 dimensional sound propagation is valid, it is a convenient environment to study the fundamental physical properties of these materials, facilitating further research considering the problem in higher dimensions. The experimental results confirm the presence of a dispersive effective bulk modulus, and within the long wavelength limit the wave number of the material is shown to have a negative gradient around the resonant region of the SHS elements. This negative group velocity suggests the material is double negative within this region. The resonant behaviour also creates large levels of attenuation across the material, suggesting the material would be effective as an acoustic isolator, and due to it's mesh design may be particularly useful in scenarios where maintaining a fluid flow renders solid isolation non-viable.

Since locally resonant designs produce materials with dispersive properties the beneficial behaviour is often limited to fixed and narrow frequency bands. As metamaterials development continues towards a commercially viable solution it will be necessary to create a higher density of resonant elements and increase the degrees of freedom. As densities increase. conventional manufacturing techniques are impractical on such scales, and additive layer manufacturing (3-dimensional printing) is likely to be a viable solution. Therefore the material presented here was designed for, and produced using, existing additive layer manufacturing techniques and methods for broadening the frequency range at which useful behaviour is achieved have been considered.

SPLIT HOLLOW SPHERE METAMATERIAL THEORY

The locally resonant acoustic metamaterial considered here is similar to that presented in [8], where an array of SHS are used as locally resonant elements. These SHS act like Helmholtz resonators, with the mass of air within the neck of the resonator acting on the compliant volume of air within the resonator cavity. SHS are analogous to the electromagnetic split ring resonators described by Pendry et al [9] and can be used to tune the effective bulk modulus of an acoustic material.

Effective Bulk Modulus

The novel effects that make acoustic metamaterials a region of research interest stem from their ability to produce negative effective material parameters. The SHS type material presented here provides a mechanism for tuning the bulk modulus of the effectively homogeneous medium. The resonant frequency of a Helmholtz resonator is

$$\omega_0 = c_0 \sqrt{\frac{S}{LV_r}} \tag{1}$$

where ρ_0 and L' are respectively the ambient density of air and the effective length of the resonator neck, c_0 is the ambient sound speed and V_r is the volume of air within the resonator cavity. When considering an array of SHS in an acoustic medium it is possible to derive an expression for the effective bulk modulus, B_e of the material [7]

$$\frac{1}{B_e} = \frac{1}{B}\left(1 - \frac{F\omega_0^2}{\omega^2 - \omega_0^2 - j\Gamma\omega}\right) \tag{2}$$

where F is the volume ratio of the SHS to the homogenous medium, and Γ is the intrinsic loss of the resonator elements. Where M different types of resonators are combined within a metamaterial, the volume ratio and resonant frequency of the mth type of resonator is calculated separately such that the effective bulk modulus becomes

$$\frac{1}{B_e} = \frac{1}{B}\left(1 - \sum_{m=1}^{M} \frac{F_m\omega_{0m}^2}{\omega^2 - \omega_{0m}^2 - j\Gamma\omega}\right) \tag{3}$$

Wave Number

The wavenumber within a medium is defined as

$$k = \frac{\omega}{c} \tag{4}$$

where c is the frequency dependent sound speed, or phase velocity. Providing the frequency of interest is much lower than that of the Bragg gap (related to the lattice spacing of the periodic elements such that the onset edge frequency $f_b = c_0/(2d_l)$ where d_l is the lattice constant) the phase velocity of the effective medium is $c = \sqrt{B_e/\rho_e}$, where ρ_e is the effective density. If the material is single negative (SNG) the solution for the wavenumber becomes complex and there is no travelling (real) wave component, only an evanescent wave and a band gap occurs in the materials transmission response. If the material exhibits simultaneously negative values for B_e and ρ_e, so is double negative (DNG), the phase velocity becomes negative real, waves propagate but now the phase velocity is anti-parallel to the group velocity [10].

Transfer Matrix

The metamaterial samples to be tested consist of varying numbers of independent layers, therefore a convenient method for modelling acoustic propagation through the material is the transfer matrix method. The relationship between the acoustic pressure, P_n and particle velocity U_n across a multiple layer material can be considered in terms of the transfer matrices, $\mathbf{T}_n$ such that

$$\begin{Bmatrix}\mathbf{P}_0\\ \mathbf{U}_0\end{Bmatrix} = \prod_{n=1}^{N} \mathbf{T}_n \cdot \begin{Bmatrix}\mathbf{P}_{N+1}\\ \mathbf{U}_{N+1}\end{Bmatrix} = \boldsymbol{\tau} \begin{Bmatrix}\mathbf{P}_{N+1}\\ \mathbf{U}_{N+1}\end{Bmatrix} \tag{5}$$

$$\mathbf{T}_n = \begin{Bmatrix} \cos(k_n d_n) & i z_n \sin(k_n d_n) \\ \dfrac{i \sin(k_n d_n)}{z_n} & \cos(k_n d_n) \end{Bmatrix} \tag{6}$$

where T_n is the transfer matrix of a single homogeneous layer, and k_n is dependent on the phase velocity, c_n, of the nth layer. Note that if the multiple layers are identical, as is the case with a periodic metamaterial, the product of transfer matrices, $\boldsymbol{\tau}$, reduces to $\mathbf{T}^N$. When a plane wave is incident on a layer, the continuity condition means that the total pressure and particle velocity at the boundary must equal the sum of the incident and reflected waves, and since the acoustic impedance can be expressed in terms of the pressure and particle velocity as $P/U = \pm z$, algebraic manipulation of Equation 5 yields expressions for the transmitted, T, and reflected, R, wave through a multilayer material.

$$T = \frac{P_t}{Pi,0} = \frac{2}{\boldsymbol{\tau}_{1,1} + \dfrac{\boldsymbol{\tau}_{1,2}}{z_{N+1}} + z_0 \boldsymbol{\tau}_{2,1} + \dfrac{z_0}{z_{N+1}} + \boldsymbol{\tau}_{2,2}} \tag{7}$$

$$R = \frac{P_{r,0}}{P_{i,0}} = \left(\boldsymbol{\tau}_{1,1} + \frac{\boldsymbol{\tau}_{1,2}}{z_{N+1}}\right) T - 1 \tag{8}$$

where the subscript (i, j) denotes the ith row and jth column of the matrix $\boldsymbol{\tau}$. The transmission loss across the material can then be defined as $20\log_{10} T$.

Experimental Sample Design

The locally resonant acoustic metamaterials have been produced to be tested in an impedance tube setup using a 4 microphone method as proposed by Song and Bolton [11]. The designs consist of individual circular samples, made up of a triangular porous mesh that contains an hexagonal array of 7 SHS hollow spheres, a schematic of the design and a photograph of a produced sample are shown in Figure 1. The mesh is to provide structural integrity only, and is designed to be, as far as possible, acoustically transparent. The samples have a thickness, T, and lattice constant, A, of 30mm. One of the future aims of this research is to produce metamaterials that have lattice constants on a micro scale, where one of the only viable production techniques is likely to be currently emerging 3-dimensional printing technologies. Therefore the samples have designed to be produced out of Polyamide 6, using existing 3D printing technology. The material specification is to produce the highest possible modulus of elasticity, to ensure that the measured results are due to the effect of the metamaterial form on the propagation of sound through the air, and not due to resilience in the polymer structure itself.

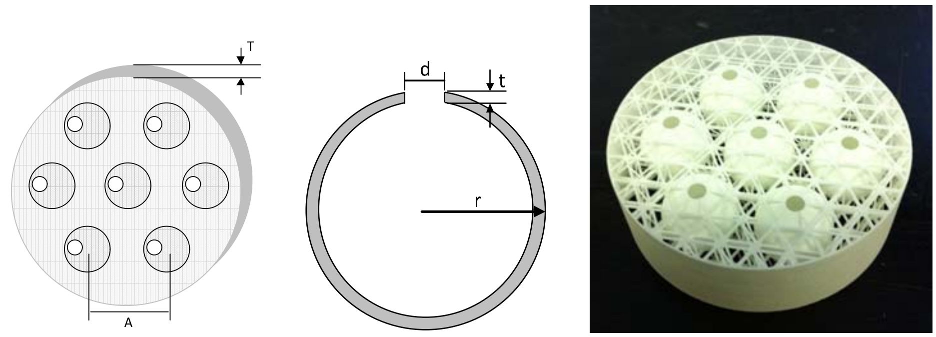

(a) (b) (c)

FIGURE 1: The schematic design of the metamaterial samples (a) the dimensions of the SHS resonators (b) and a photo of a produced metamaterial sample (c)

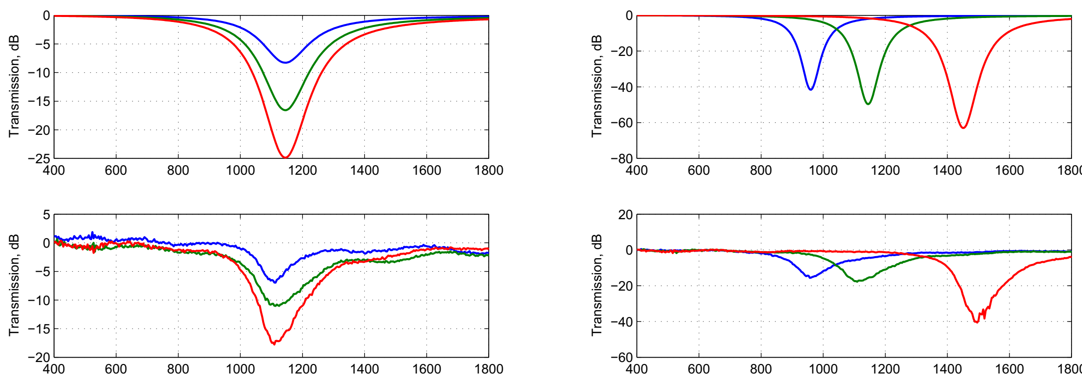

(a) (b)

FIGURE 2: (a) The transmission behaviour of 1 (blue), 2 (green) and 3 (red) layers of the 4mm resonator metamaterial, simulated (top) and measured (bottom). (b) The transmission behaviour of 2 layers of 3mm (blue), 4mm (green) and 6mm (red) resonator metamaterial, simulated (top) and measured (bottom)

In all four types of metamaterial sample were specified; three structures with arrays of SHS resonators of differing neck diameter, d, (resonator types A-C, with resonant frequencies of 960Hz, 1145Hz and 1451Hz respectively) and one structure with mixed resonators (two resonators of type A, three of type B, two of type C). In addition two control structures were specified; one a plain mesh with no SHS elements, and one with an array of solid (non resonant) spheres.

EXPERIMENTAL RESULTS

Transmission

Using the transfer matrix approach detailed in Section 2.3, it is clear that as more layers of metamaterial are added the transfer matrix, $\boldsymbol{\tau}$, is raised to a higher power such that $\boldsymbol{\tau} = \boldsymbol{T}_n^N$. There will be zeroes associated with the layer transfer matrix $\boldsymbol{T}_n$ that are responsible for the region of attenuation due to the resonator elements; the band gap. Therefore as more layers are added, the numerator equations that produce these zeroes are raised to the power N, creating additional zeros. These zeroes occupy the same location in the complex plane, which means one would expect the depth of the band gap to increase as more layers are added, but the location of the band gap in the frequency domain to remain constant. Figure 2(a) confirms this behaviour occurring in both simulations and measured results. The level of attenuation achieved is lower and the Q-factor of the notch achieved is wider in the measured results compared to the simulations. Nevertheless, the simulations do capture the general features of the material and the departure from the experimental results is due to the intrinsic losses, Γ, in the resonator elements. For the purposes of simulation this was chosen to have a fixed value of $0.08\omega_0$ to best fit the effective bulk modulus calculations with the measured results in Section 4.2. In reality, the loss behaviour is unknown and may be more accurately represented by a dispersive function.

Conversely, changing the natural frequency of the resonator elements has a direct effect on the wave number, k_d of the metamaterial, and therefore a change in the radius of the resonator neck leads to a change in the location of the resulting band gap. Figure 2(b) shows how the band gap changes location as the resonant frequency of the resonators is changed for both simulated and measured results. As a datum, mesh structures containing no resonator elements were also measured, as well as mesh structures containing solid spheres. Here the lack of resonant behaviour means that the transmission behaviour is unity (neglecting viscous losses within the tube), proving the effects seen are not due to scattering of the mesh or the spheres.

Wave number and bulk modulus

The 4 microphone technique allows one to measure not only the transmission loss but the specific acoustic impedance and the wave number of the sample under test. From this it is possible to calculate the bulk modulus. Figures 3(a) and 3(b) show the simulated and measured bulk modulus and wave number of 3 layers of a metamaterial with 4mm type resonators. The gradient of the wave number becomes negative (i.e. the group velocity is negative) around the resonant frequency of the SHS elements, a result of the dispersive bulk modulus shown. In the measurements performed the bulk modulus is inferred from the measured wave number, however in reality it is logical to consider the dispersion behaviour a consequence of the dispersive effective bulk modulus of the material. As shown in Figures 3(c) and 3(d), the effective bulk modulus and wave number remains constant with the addition of extra layers of metamaterial, as it is function of the ratio of the resonator volumes to the overall volume of the metamaterial, which will remains constant. The figures also show the wave number and bulk modulus of the plain mesh type, control material. The bulk modulus for this is shown to be approximately the ambient value for air (B_0) and the wave number to increase linearly with frequency, as expected.

The bulk modulus is shown to have a dip around resonance, in most cases measured the dip is not enough to overcome the static bulk modulus of the transmission medium and achieve negativity. Negativity could theoretically be achieved by changing the dimension/number of resonators to increase the volume ratio, F, and allow the dispersive bulk modulus component to become larger and overcome the static component.

Mixed Resonators

In the above results the desired behaviour only occurs in a narrow frequency band around the resonant frequency of the SHS. A passive route to widening this region is to create metamaterials of mixed resonator types, so the effects occur at more than one frequency. Figure 4 compares the performance of 2 such multi-resonator metamaterials, where one material has been created by using 2 identical layers that consist of a mix of resonators (2 x 3mm, 3 x 4mm, 2 x 6mm) and

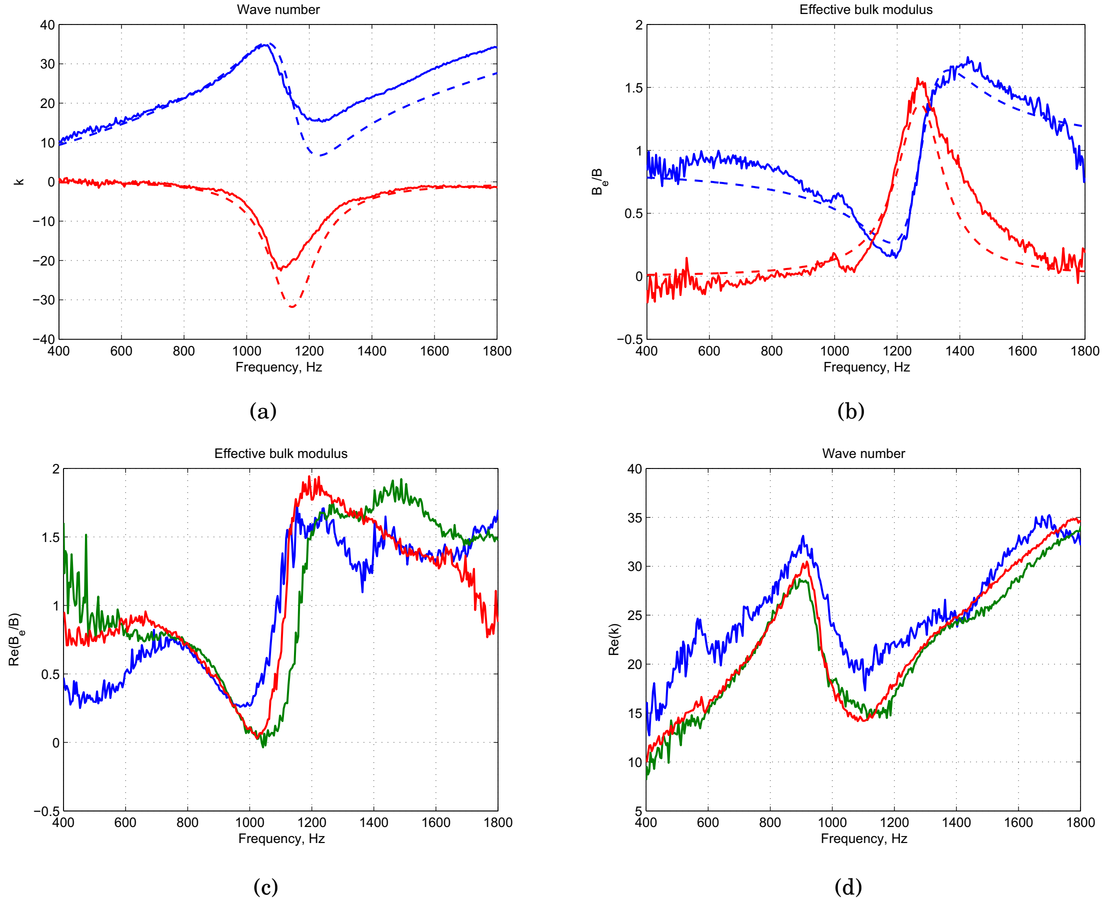

FIGURE 3: The wave number (a) and bulk modulus (b) of a 3 layer metamaterial with 4mm type resonators, real (blue) and imaginary (red). The simulated (dotted) and measured (solid) results are presented. The measured wave number (c) and bulk modulus (d) of a metamaterial of 3mm type resonators consisting of 1 (blue), 2 (red), 3 (green) layers

another has been created by using 3 distinct layers where each layer has a different resonator type. As the figures show, by mixing the resonator types the transmission blocking and effect on the bulk modulus and wave number can now be seen at multiple frequencies. If the resonator frequencies were set such that these regions overlapped then a single, wide band, region of attenuation could be expected.

The above results demonstrate the effect that the resonant elements have on the behaviour of plane waves as they travel through the metamaterial. This behaviour is due to the action of the resonator elements, and is independent of their periodicity. This is an important distinction to make, since the word metamaterial is normally used to describe a material with periodic, locally resonant elements. If it is low frequencies that are of interest, as is the case in most audio frequency ranged noise control scenarios, then the lattice constants required to take advantage of periodic Bragg effects become prohibitively large, and therefore it is only the locally resonant effects which are useful. Therefore the effects seen here can be achieved without a periodic structure.

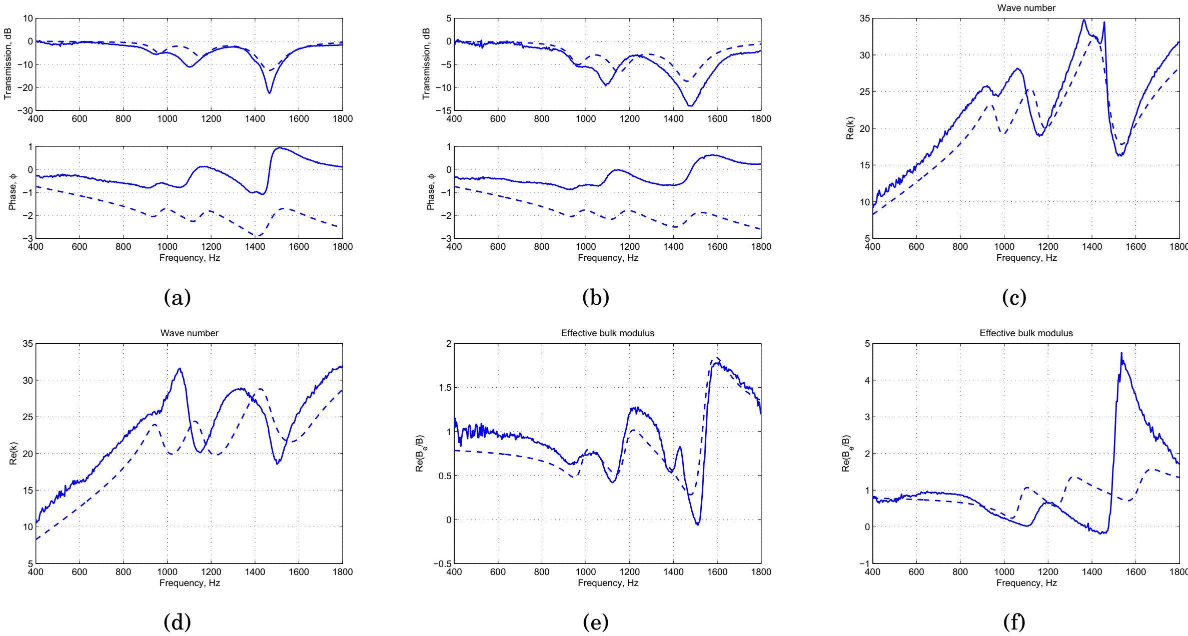

FIGURE 4: The transmission (top), wave number (middle) and bulk modulus (bottom) of a 2 layers of a mixed resonator material (left) and a 3 layer metamaterial consisting of 1 layer of each resonator type (right). Simulated (blue) and measured (green) performance

Conclusion

Various metamaterial samples consisting of SHS elements within an acoustically transparent mesh were produced and tested experimentally. The samples were shown to have a dispersive effective bulk modulus at the frequencies associated with the resonant elements, this region is also associated with attenuation of acoustic waves. The frequency range over which attenuation and dispersive B_e could be achieved can be widened passively by mixing the resonator types, providing several resonant regions that overlap. The samples have been manufactured using additive layer techniques, thereby demonstrating a feasible approach for the production of micro-scale, complex materials.

This work was carried out with funding from the EPSRC, BAE Systems and under the DSTL MAST CDE program. The metamaterials were produced by the EPSRC National Centre for Innovative Manufacturing in Additive Manufacturing, Nottingham University, with assistance of Dr Chris Tuck and Prof. Richard Hague. This support is gratefully acknowledged.

REFERENCES

[1] D. R. Smith and N. Kroll, “Negative refractive index in left-handed materials”, Physical Review Letters **85**, 2933–2936 (2000).

[2] V. Veselago, “The electrodynamics of substances with simultaneously negative values of permittivity and permeability”, Soviet Physics Uspekhi-Ussr **10**, 509–514 (1968).

[3] N. Fang, D. J. Xi, J. Y. Xu, M. Ambati, W. Srituravanich, C. Sun, and X. Zhang, “Ultrasonic metamaterials with negative modulus”, Nature Materials **5**, 452–456 (2006).

[4] Z. Y. Liu, C. T. Chan, P. Sheng, A. L. Goertzen, and J. H. Page, “Elastic wave scattering by periodic structures of spherical objects: Theory and experiment”, Physical Review B **62**, 2446–2457 (2000).

[5] Z. Y. Liu, X. X. Zhang, Y. W. Mao, Y. Y. Zhu, Z. Y. Yang, C. T. Chan, and P. Sheng, “Locally resonant sonic materials”, Science **289**, 1734–1736 (2000).

[6] H. Y. Chen and C. T. Chan, “Acoustic cloaking and transformation acoustics”, Journal of Physics D-Applied Physics **43** (2010).

[7] Y. Cheng, J. Y. Xu, and X. J. Liu, “Broad forbidden bands in parallel-coupled locally resonant ultrasonic metamaterials”, Applied Physics Letters **92** (2008).

[8] C. L. Ding and X. P. Zhao, “Multi-band and broadband acoustic metamaterial with resonant structures”, Journal of Physics D-Applied Physics **44** (2011).

[9] J. B. Pendry, A. J. Holden, D. J. Robbins, and W. J. Stewart, “Magnetism from conductors and enhanced nonlinear phenomena”, Ieee Transactions on Microwave Theory and Techniques **47**, 2075–2084 (1999).

[10] Y. Q. Ding, Z. Y. Liu, C. Y. Qiu, and J. Shi, “Metamaterial with simultaneously negative bulk modulus and mass density”, Physical Review Letters **99** (2007).

[11] B. H. Song and J. S. Bolton, “A transfer-matrix approach for estimating the characteristic impedance and wave numbers of limp and rigid porous materials”, Journal of the Acoustical Society of America **107**, 1131–1152 (2000).

[12] M. Reynolds, S. Daley, Y. Gao, V. Humphrey, and S. A. Pope, *Controller architectures for optimum performance in practical active acoustic metamaterials*, Proceedings of Acoustics 2012: 11th Congres Francais d’Acoustique and 2012 IOA annual meeting (Nantes, France) (2012).

[13] S. A. Pope and S. Daley, “Viscoelastic locally resonant double negative metamaterials with controllable effective density and elasticity”, Physics Letters A **374**, 4250–4255 (2010).

[14] W. Akl and A. Baz, “Multi-cell active acoustic metamaterial with programmable bulk modulus”, Journal of Intelligent Material Systems and Structures **21**, 541–556 (2010).